

## Nonadiabatic formulation for radiationless transitions induced by classical lattice vibrations

M. Lax

*Department of Physics, City College of the City University of New York, New York, New York 10031  
and Bell Laboratories, Murray Hill, New Jersey 07974*

H. J. Carmichael

*Center for Studies in Statistical Mechanics, University of Texas at Austin, Texas 78712*

W. J. Shugard

*Bell Laboratories, Murray Hill, New Jersey 07974*

(Received 28 January 1982; revised manuscript received 9 July 1982)

A semiclassical model for nonadiabatic radiationless transitions is described. Lattice dynamics are introduced as stochastic fluctuations in the separation and coupling of electronic levels. Formulation on the Bloch sphere brings an appealing perspective through the analogy to a magnetic moment moving in fluctuating magnetic field. Numerical solutions are reported which retain nonadiabatic features exactly. For near-adiabatic behavior, outside crossing regions, a first-order correction to adiabatic dynamics is derived and compared with the exact solution.

### I. INTRODUCTION

The capture and recombination of carriers at deep impurity levels can be of considerable importance to the operation of semiconductor devices. In particular, for semiconductor light-emitting diodes and lasers nonradiative mechanisms compete with radiative processes. For the majority of deep impurities, carrier recombination proceeds via such radiationless transitions. While the properties of shallow impurity levels are relatively well understood, nonradiative capture at deep levels remains largely an unsolved problem. Cascade capture,<sup>1-3</sup> which can account for large nonradiative cross sections at donor and acceptor sites,<sup>4</sup> cannot be invoked within the present context. Deep traps call for the disposal of an energy on the order of half the forbidden gap without the availability of the ladder of Coulomb states which mediates successive single-phonon emissions in the cascade process.

Two known mechanisms are presently proposed as plausible explanations for nonradiative capture at deeply bound states. The Auger effect,<sup>5</sup> which disposes of binding energies through the collisional excitation of a neighboring carrier, and multiphonon emission,<sup>6</sup> where binding energies are dissipated via lattice relaxation. Definitive evidence for nonradiative recombination by means of the Auger effect has been found in luminescence lifetime studies<sup>7-9</sup> although with relatively small cross sections. Recently a case for large Auger cross sections has been argued by Jaros.<sup>10</sup> The signature of the multiphonon mechanism is a thermally activated cross

section. Using the technique of capacitance spectroscopy,<sup>11-16</sup> Henry and Lang have presented strong experimental evidence for nonradiative capture via multiphonon emission.<sup>17,18</sup> These authors determine thirteen temperature-dependent capture cross sections for deep impurities in GaAs and GaP, and interpret these results within the framework of a simple theory for multiphonon emission. More recently, Narayanamurti *et al.*<sup>19</sup> have reported the direct observation of phonons generated during nonradiative capture in GaAs *p-n* junctions. This phonon-assisted mechanism is the subject of interest in our present study.

Nonradiative multiphonon transitions are commonly discussed within the context of the familiar configuration coordinate description.<sup>5,6,18,20-22</sup> Coupling of the trapped electron to a nucleus embedded in the lattice causes a horizontal displacement of the effective lattice potential associated with the bound state. In a single-coordinate picture a crossing of zeroth-order potential energy curves arises for large enough excursions from the equilibrium configuration. Radiationless transitions then involve both quantum-mechanical tunneling between lowest, energy-conserving, vibrational states (weak lattice coupling, low temperature) and activation to this crossing region (strong lattice coupling, high temperature).<sup>20,21</sup>

Multiphonon radiationless transitions have much in common with phonon-assisted radiative transitions, as both processes involve the same phonon states. Historically, both theories have often received contemporary development. However, a

fundamental distinction must be recognized. While deviations from the Born-Oppenheimer description bring only second-order corrections to optical cross sections this nonadiabatic coupling is the very source of interaction in the nonradiative case. The attitude has generally been that transition probabilities may be attributed to small deviations from adiabatic conditions. Huang and Rhys<sup>23</sup> discussed both radiative and nonradiative transitions for interaction with phonons of a single frequency, and, subsequently, their work was extended to the treatment of a general phonon spectrum.<sup>21,22,24-26</sup> In each of these formulations an adiabatic basis is adopted and transition matrix elements are calculated in the Condon approximation (Kubo and Toyozawa<sup>22</sup> include a brief discussion of non-Condon features). More recently, it has been pointed out that the strong mixing of electronic wave functions near a level crossing invalidates the Condon approximation for nonradiative transitions.<sup>27-30</sup> In a non-Condon formulation<sup>27,28</sup> Sinyavskii and Kovarskii have found increases of from 2 to 3 orders of magnitude for capture cross sections in semiconductors. They report good agreement with experimental results for numerous high-temperature cross sections in Ge and Si.<sup>28</sup> Nitzan and Jortner<sup>30</sup> have extended their method to treat nonradiative intramolecular decay in large molecules and find non-Condon corrections of a similar order.

These non-Condon calculations approach the important question of wave function mixing at a level crossing; however, the underlying Born-Oppenheimer perspective remains. Lax and Shugard<sup>31</sup> have called for a complete reexamination of the theory without a basis in the adiabatic approximation. In this paper we present preliminary results for the model proposed by these authors. The philosophy has been to begin simply by isolating nonadiabatic features while avoiding the complexities of a detailed quantum-mechanical description. Lattice dynamics are then introduced in a classical and phenomenological manner as stochastic fluctuations in the splitting and coupling between two electronic levels. With the aid of numerical procedures a full dynamical perspective on level crossings and transition events is accessible. We find that it is convenient to formulate these dynamics on the Bloch sphere where our intuition is aided by the magnetic analogy. The state of the system imitates a magnetic moment moving under the influence of an external magnetic field which fluctuates with the vibrating lattice.

Numerical results corresponding to a single realization of lattice fluctuations are discussed here.

The ultimate objective is to compare Monte Carlo estimates for transition rates with the predictions of approximate analytic results. En route to this goal, a major obstacle arises in the need to integrate rapid oscillations associated with adiabatic dynamics over near-adiabatic regions separating crossing events. A first-order correction to adiabatic dynamics has been derived to assist in overcoming this difficulty. When compared with exact numerical results this solution is a considerable improvement over an adiabatic description.

Our presentation is organized as follows. In Secs. II and III the two-level semiclassical model introduced by Lax and Shugard is described and related to dynamics on the Bloch sphere. A first-order correction to the adiabatic approximation for near-adiabatic behavior is discussed in Sec. IV. Our numerical results are presented in Sec. V. In Sec. VI we summarize this work.

## II. FORMALISM AND BACKGROUND

The mechanism for nonradiative multiphonon transitions generally involves both quantum-mechanical tunneling between low-energy vibrational states and activation to a crossing of zeroth-order potentials. A semiclassical formulation has been adopted for our present study where tunneling features are omitted. Low-temperature and weak-coupling conditions then fall outside the scope of these discussions. However, our interests lie with the nonadiabatic character of transitions. It is within the crossing region that nonadiabatic dynamics are most important and the essential content of these dynamics is retained by a semiclassical description. In view of its relative simplicity the semiclassical approach is well recommended for an initial investigation.

The work of Landau<sup>32</sup> and Zener<sup>33</sup> is well known as a classic treatment for nonadiabatic energy level crossings. A simple generalization of the Landau-Zener model has been proposed by Lax and Shugard<sup>31</sup> for studies of carrier capture at a deep trap. To set this model within context we first introduce an electronic Hamiltonian  $H(\vec{q})$  together with adiabatic eigenstates  $|\phi_n\rangle_{\vec{q}}$ . Both depend parametrically on the lattice configuration  $\vec{q}$ . If  $E_n(\vec{q})$  are the corresponding adiabatic energies, we have

$$H(\vec{q})|\phi_n\rangle_{\vec{q}} = E_n(\vec{q})|\phi_n\rangle_{\vec{q}}. \quad (2.1)$$

For some suitable reference configuration  $\vec{q}_0$  we may identify  $|1\rangle \equiv |\phi_1\rangle_{\vec{q}_0}$  and  $|2\rangle \equiv |\phi_2\rangle_{\vec{q}_0}$  with

free and bound electronic states, respectively. Then, settling for a two-level description, a general state  $|\Psi\rangle$  is expanded in this diabatic representation. It is convenient to define the associated amplitudes  $d_1$  and  $d_2$  with

$$|\Psi\rangle = e^{-i\phi(t)}(d_1|1\rangle + d_2|2\rangle), \quad (2.2)$$

where

$$\Phi(t) = \frac{1}{2\hbar} \int_0^t dt' [E_1^0(\vec{q}(t')) + E_2^0(\vec{q}(t'))] \quad (2.3)$$

has been extracted as a common phase factor. Here  $E_{1,2}^0(\vec{q})$  are zeroth-order energies,

$$E_n^0(\vec{q}) = \langle n | H(\vec{q}) | n \rangle, \quad n = 1, 2. \quad (2.4)$$

Introducing

$$J(\vec{q}) = \frac{1}{\hbar} [E_1^0(\vec{q}) - E_2^0(\vec{q})], \quad (2.5)$$

$$V(\vec{q}) = \frac{1}{\hbar} \langle 2 | H(\vec{q}) | 1 \rangle,$$

the Schrödinger equation then reads

$$\frac{d}{dt} \begin{bmatrix} d_1 \\ d_2 \end{bmatrix} = -iM_D \begin{bmatrix} d_1 \\ d_2 \end{bmatrix}, \quad (2.6)$$

$$M_D = \begin{bmatrix} \frac{J(\vec{q})}{2} & V^*(\vec{q}) \\ V(\vec{q}) & -\frac{J(\vec{q})}{2} \end{bmatrix}.$$

and corresponds to the form adopted in Ref. 31 (but the designations for states  $|1\rangle$  and  $|2\rangle$  are interchanged). Within a semiclassical scheme this equation is supplemented by a classical prescription for lattice dynamics. A specific characterization will be introduced in Sec. V and for the present an implicit time dependence in  $\vec{q}$  is to be understood.

Radiationless transitions arise with events  $J(\vec{q})=0$  corresponding to the crossing of zeroth-order energies. The special significance of these level crossings is clearly indicated within the adiabatic representation. Adiabatic states  $|\phi_1\rangle_{\vec{q}}$  and  $|\phi_2\rangle_{\vec{q}}$  may be determined via a simple matrix diagonalization. If an arbitrary phase  $\phi(\vec{q})$  is included we find

$$|\phi_1\rangle_{\vec{q}} = \frac{e^{i\phi(\vec{q})}}{\sqrt{2}} A(\vec{q})[|1\rangle + B(\vec{q})|2\rangle], \quad (2.7)$$

$$|\phi_2\rangle_{\vec{q}} = \frac{e^{-i\phi(\vec{q})}}{\sqrt{2}} A(\vec{q})[|2\rangle - B^*(\vec{q})|1\rangle], \quad (2.8)$$

with corresponding energies

$$E_{1,2}(\vec{q}) = \frac{E_1^0(\vec{q}) + E_2^0(\vec{q})}{2} \pm \frac{\hbar}{2} [J(\vec{q})^2 + 4|V(\vec{q})|^2]^{1/2}. \quad (2.9)$$

Coefficients  $A(\vec{q})$  and  $B(\vec{q})$  are given by

$$A(\vec{q}) = \left[ \frac{E_1(\vec{q}) - E_2(\vec{q})}{\hbar J(\vec{q}) + E_1(\vec{q}) - E_2(\vec{q})} \right]^{-1/2}, \quad (2.10)$$

$$B(\vec{q}) = \frac{2\hbar V(\vec{q})}{\hbar J(\vec{q}) + E_1(\vec{q}) - E_2(\vec{q})}. \quad (2.11)$$

Then expanding  $|\Psi\rangle$  as

$$|\Psi\rangle = e^{-i\Phi(t)}(a_1|\phi_1\rangle_{\vec{q}} + a_2|\phi_2\rangle_{\vec{q}}), \quad (2.12)$$

the Schrödinger equation in the adiabatic representation reads

$$\frac{d}{dt} \begin{bmatrix} a_1 \\ a_2 \end{bmatrix} = -iM_A \begin{bmatrix} a_1 \\ a_2 \end{bmatrix}, \quad (2.13)$$

with

$$M_A = \begin{bmatrix} \frac{E_1(\vec{q}) - E_2(\vec{q})}{2\hbar} & 0 \\ 0 & -\frac{E_1(\vec{q}) - E_2(\vec{q})}{2\hbar} \end{bmatrix} + [\epsilon_{ij}(\vec{q}, \dot{\vec{q}})], \quad (2.14)$$

where

$$\epsilon_{ij}(\vec{q}, \dot{\vec{q}}) = -i_{\vec{q}} \left\langle \phi_i \left| \sum_k \dot{q}_k \frac{\partial}{\partial q_k} \right| \phi_j \right\rangle_{\vec{q}}, \quad (2.15)$$

Using Eqs. (2.7)–(2.11) it is readily shown that the matrix  $(\epsilon_{ij})$  is Hermitian with  $\epsilon_{11} = -\epsilon_{22}$ .

In Eq. (2.13) an explicit coupling of adiabatic states enters through the perturbation  $\epsilon_{12}$ , where, using Eq. (2.1) we may write

$$\epsilon_{12}(\vec{q}, \dot{\vec{q}}) = -i_{\vec{q}} \left\langle \phi_1 \left| \left[ \sum_k \dot{q}_k \frac{\partial}{\partial q_k} H(q) \right] \right| \phi_2 \right\rangle_{\vec{q}} \frac{1}{E_1(\vec{q}) - E_2(\vec{q})}. \quad (2.16)$$

The strength of this nonadiabatic coupling is then

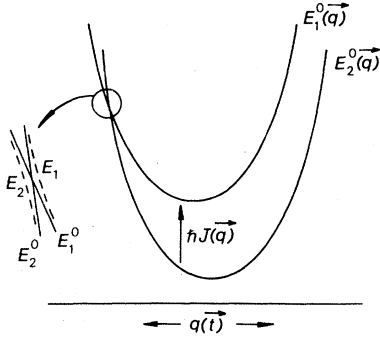


FIG. 1. One-dimensional configuration coordinate diagram illustrating the crossing of zeroth-order energies.

measured, to a first approximation, by the ratio

$$\begin{aligned} \Gamma &= 2\hbar \frac{|\epsilon_{12}(\vec{q}, \dot{\vec{q}})|}{E_1(\vec{q}) - E_2(\vec{q})} \\ &= 2\hbar \frac{\left| \left\langle \phi_1 \right| \left[ \sum_k \dot{q}_k \frac{\partial}{\partial q_k} H(\vec{q}) \right] \left| \phi_2 \right\rangle \right|_q}{[E_1(\vec{q}) - E_2(\vec{q})]^2} \end{aligned} \quad (2.17)$$

The significance of the crossing region derives from the dependence on  $E_1 - E_2$ . A crossing of zeroth-order energies has  $J = E_1^0 - E_2^0 = 0$ . Adiabatic energies are repelled at the crossing (see Fig. 1) so that the divergence in  $\Gamma$  is removed. Nevertheless, at their closest approach  $\Gamma$  is significantly enhanced.

Of course, exact solutions to Eqs. (2.6) and (2.13) provide equivalent results. We should recognize however, that within these separate contexts approximate schemes based on first-order perturbation theory presuppose quite different dynamics. The standard approach<sup>20-30</sup> sees a small departure from adiabatic dynamics as the basis for transitions and development begins with Eq. (2.13) (the Condon approximation takes  $\epsilon_{12}$  constant). In contrast, Henry and Lang<sup>18</sup> match a region of adiabatic dynamics to a sudden approximation close to the crossing. Transitions arise in the region of sudden dynamics where diabatic states provide a natural basis and perturbation theory is then employed within the context of Eq. (2.6) ( $V$  is taken constant and equal to its value at the crossing). Lax and Shugard<sup>31</sup> have also calculated transition rates in a perturbative approach. Again the theory is founded in Eq. (2.6). Near-adiabatic and near-sudden approximations present diametrically opposed perspectives on the dynamics of electron capture, and this comparison only serves to underline the need for a full, nonperturbative, understanding of crossing events.

### III. BLOCH FORMULATION AND THE MAGNETIC ANALOGY

The numerical simulations reported in Sec. V correspond to the solution of Eq. (2.6) for a stochastic realization of lattice dynamics. However, rather than working with complex amplitudes we have chosen to make a transformation to the Bloch sphere. Beyond its computational convenience, the Bloch formulation offers a simple intuitive perspective on nonadiabatic dynamics. In this section we outline the relationship between Schrödinger and Bloch sphere. For simplicity, we drop the explicit  $\vec{q}$  notation, and in its place an implicit time dependence is to be understood.

The formal equivalence between a two-state system and spin dynamics is well known, and widely exploited in discussions of radiative processes.<sup>34</sup> We review only essential features here. At the outset let us adopt diabatic states as a basis. We introduce Pauli operators  $\sigma_{\pm}^{(d)} = \sigma_x^{(d)} \pm i\sigma_y^{(d)}$  and  $\sigma_z^{(d)}$ , where

$$\begin{pmatrix} \sigma_+^{(d)} \\ \sigma_-^{(d)} \\ \sigma_z^{(d)} \end{pmatrix} = K \begin{pmatrix} \sigma_x^{(d)} \\ \sigma_y^{(d)} \\ \sigma_z^{(d)} \end{pmatrix} = \begin{pmatrix} |1\rangle\langle 2| \\ |2\rangle\langle 1| \\ |1\rangle\langle 1| - |2\rangle\langle 2| \end{pmatrix}, \quad (3.1)$$

with

$$K = \frac{1}{2} \begin{pmatrix} 1 & i & 0 \\ 1 & -i & 0 \\ 0 & 0 & 2 \end{pmatrix}. \quad (3.2)$$

Then a general state  $|\Psi\rangle$  is identified with the vector

$$\vec{\sigma}_d = \begin{pmatrix} x_d \\ y_d \\ z_d \end{pmatrix} = \begin{pmatrix} \langle \sigma_x^{(d)} \rangle \\ \langle \sigma_y^{(d)} \rangle \\ \langle \sigma_z^{(d)} \rangle \end{pmatrix} = \begin{pmatrix} d_1 d_2^* + d_1^* d_2 \\ i(d_1 d_2^* - d_1^* d_2) \\ |d_1|^2 - |d_2|^2 \end{pmatrix}. \quad (3.3)$$

Here  $\langle \sigma \rangle$  denotes the average  $\langle \Psi | \sigma | \Psi \rangle$ . Conservation of probability ( $\langle \Psi | \Psi \rangle = 1$ ) requires  $\vec{\sigma}_d \cdot \vec{\sigma}_d = 1$  and an arbitrary state is mapped to a point on the surface of the unit (Bloch) sphere. The diabatic representation establishes a fixed coordinate system  $(x, y, z)_d \equiv (x_d, y_d, z_d)$  (the diabatic frame) to which points on the Bloch sphere are referred. Diabatic states themselves are set at the poles  $(0, 0, \pm 1)_d$ .

Dynamical evolution is now visualized in terms of trajectories on the Bloch sphere. The Bloch

equations, which describe this evolution, follow from the transformation of the Schrödinger equation. In particular, if we remain with the diabatic representation, the transformation specified by Eq. (3.3) leads from Eq. (2.6) to

$$\frac{d\vec{\sigma}_d}{dt} = N_D \vec{\sigma}_d = \vec{I}_D \times \vec{\sigma}_d, \quad (3.4)$$

where

$$\vec{I}_D = \lambda \begin{pmatrix} \sin\theta & \cos\psi \\ \sin\theta & \sin\psi \\ \cos\theta & \end{pmatrix}, \quad (3.5)$$

with

$$\begin{aligned} J &= \lambda \cos\theta, \quad 0 \leq \theta \leq \pi, \\ 2V &= \lambda \sin\theta e^{i\psi}, \quad 0 \leq \psi \leq 2\pi. \end{aligned} \quad (3.6)$$

The matrix  $N_D$  is defined through its relation to  $\vec{I}_D$ . Formally,  $\vec{\sigma}_d$  imitates the motion of a magnetic moment under the influence of a magnetic field  $\vec{I}_D$ . Our new characterization for  $J$  and  $V$  [Eq. (3.6)] is motivated to provide a polar notation for this "field." Its magnitude  $\lambda = [J^2 + 4|V|^2]^{1/2}$  and orientation  $(\theta, \psi)$  both fluctuate with the vibrating lattice.

Orthonormal bases are related by a rotation of coordinates on the Bloch sphere. Specifically, if adiabatic states are represented by  $\vec{\sigma}_d^{\phi_1}$  and  $\vec{\sigma}_d^{\phi_2}$  in diabatic coordinates, then, from Eqs. (2.7) and (2.8), we readily find

$$\begin{aligned} \vec{\sigma}_d^{\phi_1} &= \begin{pmatrix} \sin\theta & \cos\psi \\ \sin\theta & \sin\psi \\ \cos\theta & \end{pmatrix}, \\ \vec{\sigma}_d^{\phi_2} &= \begin{pmatrix} \sin(\pi+\theta) & \cos\psi \\ \sin(\pi+\theta) & \sin\psi \\ \cos(\pi+\theta) & \end{pmatrix}. \end{aligned} \quad (3.7)$$

Adiabatic states lie at antipodes along the axis of the field  $\vec{I}_D$ . Equations (3.1) and (3.3) might now be translated into analogous definitions with the adiabatic states, as a basis. We introduce, in corresponding notation, the operators  $\sigma_{\pm}^{(a)} = \sigma_x^{(a)} \pm i\sigma_y^{(a)}, \sigma_z^{(a)}$  and the vector representation  $\vec{\sigma}_a$ . Choosing a phase  $\phi(\vec{q}) = -\psi/2$  in Eqs. (2.7) and (2.8) it is easily shown that

$$\sigma_a = R_y(\theta)R_z(\psi)\sigma_d, \quad (3.8)$$

where

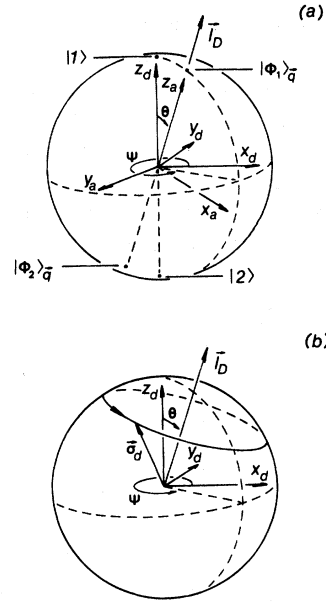


FIG. 2. Representation of electronic states on the Bloch sphere: (a) diabatic and adiabatic coordinates, (b) precession of  $\vec{\sigma}_d$  about  $\vec{I}_D$  in adiabatic dynamics.

$$\begin{aligned} R_y(\theta) &= \begin{pmatrix} \cos\theta & 0 & -\sin\theta \\ 0 & 1 & 0 \\ \sin\theta & 0 & \cos\theta \end{pmatrix}, \\ R_z(\psi) &= \begin{pmatrix} \cos\psi & \sin\psi & 0 \\ -\sin\psi & \cos\psi & 0 \\ 0 & 0 & 1 \end{pmatrix}, \end{aligned} \quad (3.9)$$

are standard rotation matrices.<sup>35</sup> Adiabatic coordinates  $(x, y, z)_a \equiv (x_a, y_a, z_a)$  are rotated from the diabatic frame to set the  $z_a$  axis parallel to  $\vec{I}_D$ . The full geometry is illustrated in Fig. 2(a).

Dynamical features follow the intuition derived within this magnetic analogy. Beginning with Eq. (3.4), the matrix  $N_D$  is diagonalized by a similarity transformation,

$$KQ^{-1}N_DQK^{-1} = \begin{pmatrix} i\lambda & 0 & 0 \\ 0 & -i\lambda & 0 \\ 0 & 0 & 0 \end{pmatrix} = \Lambda, \quad (3.10)$$

where

$$Q^{-1} = R_y(\theta)R_z(\psi), \quad (3.11)$$

and

$$KQ^{-1}\vec{\sigma}_d = K\vec{\sigma}_a = \begin{pmatrix} \langle \sigma_+^{(a)} \rangle \\ \langle \sigma_-^{(a)} \rangle \\ \langle \sigma_z^{(a)} \rangle \end{pmatrix}. \quad (3.12)$$

This sets us in the adiabatic frame. The matrix  $K$  merely identifies rotating variables. Then, if  $\theta$  and  $\psi$  remain fixed in time, rotating solutions in adiabatic coordinates correspond to the precession of  $\vec{\sigma}_d$  about  $\vec{\Gamma}_D$ . However, our interests lie with a fluctuating lattice, where  $\theta$  and  $\psi$  are not constant. The movement of adiabatic coordinates must then be considered. From Eqs. (3.4) and (3.8) we find

$$\frac{d\vec{\sigma}_d}{dt} = N_A \vec{\sigma}_d = \vec{\Gamma}_A \times \vec{\sigma}_d, \quad (3.13)$$

where

$$\vec{\Gamma}_A = \begin{pmatrix} \dot{\psi} \sin \theta \\ -\dot{\theta} \\ \lambda - \dot{\psi} \cos \theta \end{pmatrix}, \quad (3.14)$$

and the matrix  $N_A$  is defined through its relation to  $\vec{\Gamma}_A$ . As we must expect, Eq. (3.13) corresponds to the transformation from Eq. (2.13) to the Bloch sphere. Terms in  $\theta$  and  $\psi$  are identified with the nonadiabatic contribution ( $\epsilon_{ij}$ ). Their introduction here moves the field  $\vec{\Gamma}_A$  from its alignment with the  $z$  axis and the equation in  $K\vec{\sigma}_d$  is no longer diagonal.

An adiabatic approximation to the solution of Eq. (3.13) might be made if  $\dot{\theta}$  and  $\dot{\psi}$  are sufficiently small. We approximate  $\vec{\sigma}_d$  by

$$\vec{\sigma}_d^{(\text{adb})}(t) = Q(t) R_z \left[ - \int_0^t dt' \lambda(t') \right] Q^{-1}(0) \vec{\sigma}_d(0), \quad (3.15)$$

and  $\vec{\sigma}_d$  follows the field  $\vec{\Gamma}_D$  while precessing about its instantaneous direction [(Fig. 2(b)). Here  $Q(t)$  is defined by Eq. (3.11) with  $\theta$  and  $\psi$  replaced by their time-dependent values  $\theta(t)$  and  $\psi(t)$ . Our intuition indicates that the criterion for such behavior must require the angular frequency for precession  $\lambda$  to remain much larger than the maximum frequency governing movement in  $\vec{\Gamma}_D$ . Since nonadiabatic coupling enters Eq. (3.13) as a misalignment of the field  $\vec{\Gamma}_A$ , a measure of this coupling strength is given by the ratio

$$\bar{\Gamma} = \left[ \frac{\vec{\Gamma}_A \cdot \vec{\Gamma}_A - (\vec{\Gamma}_A \cdot \hat{z}_a)^2}{\vec{\Gamma}_A \cdot \vec{\Gamma}_A} \right]^{1/2}, \quad (3.16)$$

where  $\hat{z}_a$  is a unit vector along the  $z_a$  axis. We find

$$\bar{\Gamma} = \frac{1}{\lambda} (\dot{\theta}^2 + \dot{\psi}^2 \sin^2 \theta)^{1/2}, \quad (3.17)$$

with

$$\bar{\lambda} = [(J - \dot{\psi})^2 + 4|V|^2 + \theta^2]^{1/2}. \quad (3.18)$$

Here  $\bar{\lambda}$  includes nonadiabatic corrections to the precession frequency, where, as we recall, the adiabatic frequency  $\lambda = [J^2 + 4|V|^2]^{1/2}$ . Apart from this adjustment  $\bar{\Gamma}$  corresponds precisely to Eq. (2.17). Energy-level crossings appear as agents which slow the precession of  $\vec{\sigma}_d$  and reduce the potential for adiabatic following. If  $\bar{\Gamma} \ll 1$  is adopted as a criterion for adiabatic dynamics, it is readily shown that fulfillment of this condition within the crossing region  $J \approx \dot{\psi}$  requires

$$\frac{\dot{\theta}}{2|V|}, \frac{\dot{\psi}}{2|V|} \ll 1. \quad (3.19)$$

Note that the crossing has been moved from  $J=0$  to  $J=\dot{\psi}$ . This comes with the inclusion of nonadiabatic corrections to the adiabatic frequency  $\lambda$ , and reflects the tuning of lattice modes to the electronic levels (for  $\psi = \omega t$ ,  $V = |V| e^{i\omega t}$ ). Corrections to adiabatic dynamics are pursued in more detail in the following section.

#### IV. CORRECTIONS TO ADIABATIC DYNAMICS

The transformation from diabatic to adiabatic coordinates provides a natural route to the solution of Eq. (3.4) if  $\dot{\theta} = \dot{\psi} = 0$ . More generally it may still represent an approach towards this solution. In particular, the adiabatic response given by Eq. (3.15) is surely a good approximation for  $\dot{\theta}/\bar{\lambda} \ll 1$ ,  $\dot{\psi}/\bar{\lambda} \ll 1$ . Here we present a formal scheme for generating a sequence of nonadiabatic corrections to this zeroth-order approximation. Specific attention is given to first-order results where an explicit prescription is available. In the following section these are compared with exact numerical calculations.

First we note that a simple improvement over Eq. (3.15) can be made, if, rather than dropping all terms in  $\dot{\theta}$  and  $\dot{\psi}$  from Eq. (3.14), we retain the  $z_a$  component of the field  $\vec{\Gamma}_A$  as  $\lambda - \dot{\psi} \cos \theta$ . In place of Eq. (3.15) we write

$$\begin{aligned} \vec{\sigma}_d^{(\text{adb})}(t) = Q(t) R_z \left[ - \int_0^t dt' [\lambda(t') - \dot{\psi}(t') \right. \\ \left. \times \cos \theta(t')] \right] \\ \times Q^{-1}(0) \vec{\sigma}_d(0). \end{aligned} \quad (4.1)$$

Beyond this, within our magnetic analogy the transformation to adiabatic coordinates is motivated to achieve alignment with  $\vec{\Gamma}_D$ . As we have seen in Eq. (3.14), for time-dependent fields a nonadiabatic perturbation arises to defeat this purpose. Nevertheless, the formal structure of the dynamical

equations is preserved, and it is clear then that the procedure relating diabatic and adiabatic frames may be iterated. In this fashion we might chase the field  $\vec{\Gamma}_D$  through a series of coordinate rotations. Specifically, at zeroth-order we identify (in one-to-one correspondence)

$$\begin{bmatrix} \vec{\sigma}_d, \lambda, \theta, \psi \\ \vec{\Gamma}_A, N_A, Q, \Lambda \end{bmatrix} = \begin{bmatrix} \vec{\sigma}_0, \lambda_0, \theta_0, \psi_0 \\ \vec{\Gamma}_0, N_0, Q_0, \Lambda_0 \end{bmatrix}. \quad (4.2)$$

Then, following the form of Eqs. (3.5), (3.8), and (3.14) we define

$$\vec{\sigma}_n = R_y(\theta_n)R_z(\psi_n)\sigma_{n-1}, \quad n=0,1,2,\dots, \quad (4.3)$$

with

$$\theta_n = \tan^{-1} \frac{(\dot{\theta}_{n-1}^2 + \dot{\psi}_{n-1}^2 \sin^2 \theta_{n-1})^{1/2}}{\lambda_{n-1} - \dot{\psi}_{n-1} \cos \theta_{n-1}}, \quad 0 \leq \theta_n \leq \pi, \quad n=1,2,\dots, \quad (4.4)$$

$$e^{i\psi_n} = \frac{\dot{\psi}_{n-1} \sin \theta_{n-1} - i \dot{\theta}_{n-1}}{(\dot{\theta}_{n-1}^2 + \dot{\psi}_{n-1}^2 \sin^2 \theta_{n-1})^{1/2}}, \quad 0 \leq \psi_n < 2\pi, \quad n=1,2,\dots, \quad (4.5)$$

and

$$\lambda_n = [(\lambda_{n-1} - \dot{\psi}_{n-1} \cos \theta_{n-1})^2 + \dot{\theta}_{n-1}^2 + \dot{\psi}_{n-1}^2 \sin^2 \theta_{n-1}]^{1/2}, \quad n=1,2,\dots \quad (4.6)$$

$\lambda_0$ ,  $\theta_0$ , and  $\psi_0$  are defined through Eq. (3.6). For dynamical equations at the  $n$ th order we have

$$\vec{\sigma}_d^{(n)'}(t) = \left[ \prod_{k=0}^n Q_k(t) R_z \left[ - \int_0^t dt' [\lambda_n(t') - \dot{\psi}_n(t') \cos \theta_n] \right] Q_k^{-1}(0) \prod_{k=0}^n \right] \vec{\sigma}_d(0), \quad n=0,1,2,\dots, \quad (4.11)$$

where  $\vec{\sigma}_d^{(0)'} \equiv \vec{\sigma}_d^{(\text{adb})}$ . Matrix products are to be ordered to the right and left of the product sign as indicated. Of course rotations preserve the magnitude of  $\vec{\sigma}_d$  and we readily show that  $\vec{\sigma}_d^{(n)'} \cdot \vec{\sigma}_d^{(n)'} = 1$ . If the term  $\dot{\psi}_n \cos \theta_n$  is also dropped from Eq. (4.8) we defined  $\vec{\sigma}_d^{(n)}$ , with  $\vec{\sigma}_d^{(0)} \equiv \vec{\sigma}_d^{(\text{adb})}$ , as the corresponding generalization of Eq. (3.15).

Various formal questions arise concerning this procedure. For example, what are the convergence properties for the sequence  $\vec{\sigma}_d^{(n)'}$ ? Clearly we would expect near-adiabatic and near-sudden dynamics to be distinguished in this respect. Further, what is

$$\frac{d\vec{\sigma}_n}{dt} = N_n \vec{\sigma}_n = \vec{\Gamma}_n \times \vec{\sigma}_n, \quad n=0,1,2,\dots, \quad (4.7)$$

where

$$\vec{\Gamma}_n = \begin{bmatrix} \dot{\psi}_n \sin \theta_n \\ -\dot{\theta}_n \\ \lambda_n - \dot{\psi}_n \cos \theta_n \end{bmatrix}, \quad n=0,1,2,\dots, \quad (4.8)$$

and  $N_n$  is defined through its relation to  $\vec{\Gamma}_n$ . We should note the appearance of terms  $\theta_{n-1}$  and  $\psi_{n-1}$  in Eqs. (4.4)–(4.6). These equations do not define a closed iteration scheme. Generally  $\lambda_n$ ,  $\theta_n$ , and  $\psi_n$  find explicit definition in terms of  $\lambda_0$ ,  $\theta_0$ , and  $\psi_0$ , together with  $\dot{\lambda}_0$  (beyond first order) and up to the  $n$ th-order derivatives of  $\theta_0$  and  $\psi_0$ .

We now generalize the route to Eq. (4.1) and define an  $n$ th-order approximation to the solution of Eq. (3.4). Corresponding to the definition of  $Q_0$  and  $\Lambda_0$  in Eqs. (3.10) and (3.11) we write

$$KQ_n^{-1}N_{n-1}Q_nK^{-1} = \begin{bmatrix} i\lambda_n & 0 & 0 \\ 0 & -i\lambda_n & 0 \\ 0 & 0 & 0 \end{bmatrix} = \Lambda_n, \quad n=1,2,\dots, \quad (4.9)$$

where

$$Q_n^{-1} = R_y(\theta_n)R_z(\psi_n), \quad n=1,2,\dots \quad (4.10)$$

Here  $KN_nK^{-1}$  differs from  $\Lambda_n$  only through terms in  $\theta_n$  and  $\psi_n$ . Then, dropping the terms  $\dot{\psi}_n \sin \theta_n$  and  $-\dot{\theta}_n$  from Eq. (4.8) we solve diagonal equations for  $K\vec{\sigma}_n$  and write

the relationship between this procedure and the usual perturbation theory? We will not pursue these questions in the present paper, however, and restrict our further discussion to first-order results. Here numerical calculations show that for near-adiabatic dynamics we gain considerable improvement over Eq. (3.5).

For zeroth-order variables let us return to the notation of Sec. III. Corresponding variables at first order will be identified by an overbar. Then from Eqs. (4.11), (4.4), and (4.5) an explicit prescription for  $\vec{\sigma}_d^{(1)'}$  is given by

$$\vec{\sigma}_d^{(1)'}(t) = Q(t)\bar{Q}(t)R_z \left[ - \int_0^t dt' [\bar{\lambda}(t') - \dot{\bar{\psi}}(t') \cos \bar{\theta}(t')] \right] \bar{Q}^{-1}(0)Q^{-1}(0)\vec{\sigma}_d(0), \quad (4.12)$$

where

$$\bar{Q}^{-1}Q^{-1} = R_y(\bar{\theta})R_z(\bar{\psi})R_y(\theta)R_z(\psi), \quad (4.13)$$

with

$$\cos\bar{\theta} = \frac{\lambda - \dot{\psi} \cos\theta}{\bar{\lambda}}, \quad (4.14)$$

$$\sin\bar{\theta} = \frac{(\dot{\theta}^2 + \dot{\psi}^2 \sin^2\theta)^{1/2}}{\bar{\lambda}},$$

$$\cos\bar{\psi} = \frac{\dot{\psi} \sin\theta}{(\dot{\theta}^2 + \dot{\psi}^2 \sin^2\theta)^{1/2}}, \quad (4.15)$$

$$\sin\bar{\psi} = \frac{-\dot{\theta}}{(\dot{\theta}^2 + \dot{\psi}^2 \sin^2\theta)^{1/2}},$$

and Eq. (4.6) defines  $\bar{\lambda}$  to correspond to Eq. (3.18). Here some comments are in order. Terms in  $\bar{\theta}$  and  $\bar{\psi}$  are neglected in Eq. (4.12). For  $\bar{\psi}$  we find

$$\dot{\bar{\psi}} = \frac{(\ddot{\theta}\dot{\psi} - \dot{\theta}\ddot{\psi})\sin\theta + \dot{\theta}^2\dot{\psi}\cos\theta}{\dot{\theta}^2 + \dot{\psi}^2\sin^2\theta}. \quad (4.16)$$

Note, then, that  $\bar{\sigma}_d^{(1)'} is not an exact solution for linear  $\theta$  and  $\psi$  as the Landau-Zener solution<sup>32,33</sup> is exact for linear  $J$ . Even for  $\dot{\theta} = \dot{\psi} = 0$ , Eq. (4.16) retains a term involving first derivatives. Generally similar terms will be included at all orders; increasing order bringing higher powers in these derivatives. The expression for  $\bar{\theta}$  is more cumbersome; here  $\bar{\lambda}$  also enters. Rather than give its general form we consider special cases with either  $\lambda$  and  $\theta$ , or  $\psi$ , held constant (note that while  $\lambda$  and  $\theta$  may be fixed independently, such conditions are somewhat contrived). We find for  $\lambda$  and  $\theta$  constant,$

$$\dot{\bar{\theta}} = \frac{2|V|}{(J - \dot{\psi})^2 + 4|V|^2} \ddot{\psi}, \quad (4.17)$$

and for  $\psi$  constant,

$$\dot{\bar{\theta}} = \frac{\lambda\ddot{\theta} - \lambda\dot{\theta}}{\lambda^2 + \dot{\theta}^2}. \quad (4.18)$$

Equation (4.18) again retains a term in first derivatives if  $\dot{\theta} = 0$ . On the other hand, in Eq. (4.17)  $\bar{\theta}$  vanishes with  $\dot{\psi}$ ; moreover, for constant  $\lambda$  and  $\theta$ , Eq. (4.16) gives  $\dot{\bar{\psi}} = 0$ . The special conditions  $\lambda = \theta = \psi = 0$  are then treated exactly in Eq. (4.12). This is no surprise, since with  $\psi = \omega$  and  $\dot{\psi} = 0$ , we have  $V = |V|e^{i\omega t}$ . A single-frequency rotating interaction is traditionally treated by adopting a rotating frame, where in Eq. (2.6)  $V \rightarrow |V|$  and  $J \rightarrow J - \omega$ . This transformation is readily recovered from Eq. (4.12). Since  $\dot{\theta} = 0$ , Eq. (4.15) has  $\bar{\psi} = 0$  and  $\bar{\psi} = \pi$  for  $\dot{\psi} > 0$  and  $\dot{\psi} < 0$ , respectively. Using

$$R_y(\bar{\theta})R_z(\pi) = R_z(\pi)R_y(-\bar{\theta})$$

in the latter case, Eq. (4.12) gives

$$\bar{\sigma}_d^{(1)'}(t) = Q_\omega(t)R_z(-\bar{\lambda}t)Q_\omega^{-1}(0)\bar{\sigma}_d(0), \quad (4.19)$$

where

$$Q_\omega^{-1}(t) = R_y(\theta + \text{sgn}(\omega)\bar{\theta})R_z(\omega t), \quad (4.20)$$

$$\bar{\lambda} = [(J - \omega)^2 + 4|V|^2]^{1/2}.$$

Here,  $R_z(\omega t)$  introduces the usual rotating frame, and, while

$$\theta = \tan^{-1} \left[ \frac{2|V|}{J} \right], \quad 0 \leq \theta \leq \pi, \quad (4.21)$$

from Eq. (4.14) we find

$$\theta + \text{sgn}(\omega)\bar{\theta} = \tan^{-1} \left[ \frac{2|V|}{J - \omega} \right], \quad (4.22)$$

$$0 \leq \theta + \text{sgn}(\omega)\bar{\theta} \leq \pi.$$

## V. LATTICE DYNAMICS AND NUMERICAL RESULTS

Our numerical studies are based on Eq. (3.4) with an explicit time dependence introduced to  $\bar{I}_D$  to model lattice dynamics. Lax and Shugard<sup>31</sup> propose that  $J(t)$  and  $V(t) = V_1(t) + iV_2(t)$  be characterized by three independent, stationary, stochastic processes. Each process is Gaussian and, most importantly, not of the white-noise type. First moments are given by

$$\langle J(t) \rangle_s = \omega_0, \quad \delta J(t) = J(t) - \omega_0, \quad (5.1)$$

and

$$\langle V(t) \rangle_s = \langle V_1(t) \rangle_s + i \langle V_2(t) \rangle_s = 0, \quad (5.2)$$

where the angular brackets with a subscript "s" denote an average over stochastic variables, distinct from the quantum average (unadorned angular brackets) introduced in Sec. III. Equation (5.2) asserts that diabatic states are referred to an equilibrium lattice configuration— $\bar{q}_0$  in the notation of Sec. II. In Eq. (5.1),

$$\omega_0 = [E_1^0(\bar{q}_0) - E_2^0(\bar{q}_0)]/\hbar$$

is the "optical" frequency.

Nonwhite fluctuations are required to account for the frequency cutoff in the density of phonon states. This feature is of course central to the character of multiphonon transitions, where, if  $\omega_M$  denotes a

maximum phonon frequency, we have

$$\omega_M \ll \omega_0. \quad (5.3)$$

In the simulations reported here we have taken power spectra  $\phi_J(\omega)$  and  $\phi_{V_{1,2}}(\omega)$  to be flat between  $\pm\omega_M$ , with

$$\langle \delta J(t) \delta J(0) \rangle_s = \frac{1}{2\pi} \int_{-\infty}^{\infty} \phi_J(\omega) e^{i\omega t} d\omega, \quad (5.4)$$

$$\langle V_k(t) V_k(0) \rangle_s = \frac{1}{2\pi} \int_{-\infty}^{\infty} \phi_{V_k}(\omega) e^{i\omega t} d\omega, \quad (5.5)$$

$k=1,2.$

For the remaining second moments, recall that  $\delta J(t)$ ,  $V_1(t)$ , and  $V_2(t)$  are independent.

This modeling for the lattice includes the essential features underlying nonradiative capture in a simple prescription. It provides a valid context within which to study the nonadiabatic character of transitions. One feature which has been omitted, however, deserves a mention. In the above description the lattice evolves independently of the electronic state. More correctly a coupling should be introduced via the energy  $\langle \Psi | H(\vec{q}) | \Psi \rangle$ . This is clear if we consider the lattice fluctuations for ei-

ther a pure bound or pure free state. The relaxation of the lattice equilibrium following electron capture (Fig. 1) requires a different  $\omega_0$  in these two situations.

In the Bloch formulation, transition probabilities are followed in the evolution of the population difference  $\langle \vec{\sigma}_z^{(d)}(t) \rangle$  [alternatively  $\langle \vec{\sigma}_z^{(a)}(t) \rangle$ ]. Our ultimate objective in this study is to determine captures rates through the numerical calculation of  $\langle \langle \vec{\sigma}_z^{(d)}(t) \rangle \rangle_s$ . Work in this direction is still in progress. Here we report on initial results illustrating dynamics for a single realization of  $J(t)$  and  $V(t)$ .

The stochastic processes  $\delta J(t)$  and  $V_{1,2}(t)$  have been generated numerically, and Eq. (3.4) was then integrated with  $J(t)$  and  $V(t)$  explicitly prescribed. In Fig. 3 we have plotted a typical result for a system initially prepared in its upper state. For reference  $\delta J(t)$  and  $V_{1,2}(t)$  are also displayed. Note that parameters are chosen for computational convenience and to illustrate nonadiabatic effects. It is not suggested that they correspond to observed trapping conditions. We may identify three main features in this solution. First, and most obvious, are the rapid oscillations corresponding to the precession of the vector  $\vec{\sigma}_d$  about  $\hat{1}_D$  (Fig. 2). These represent only

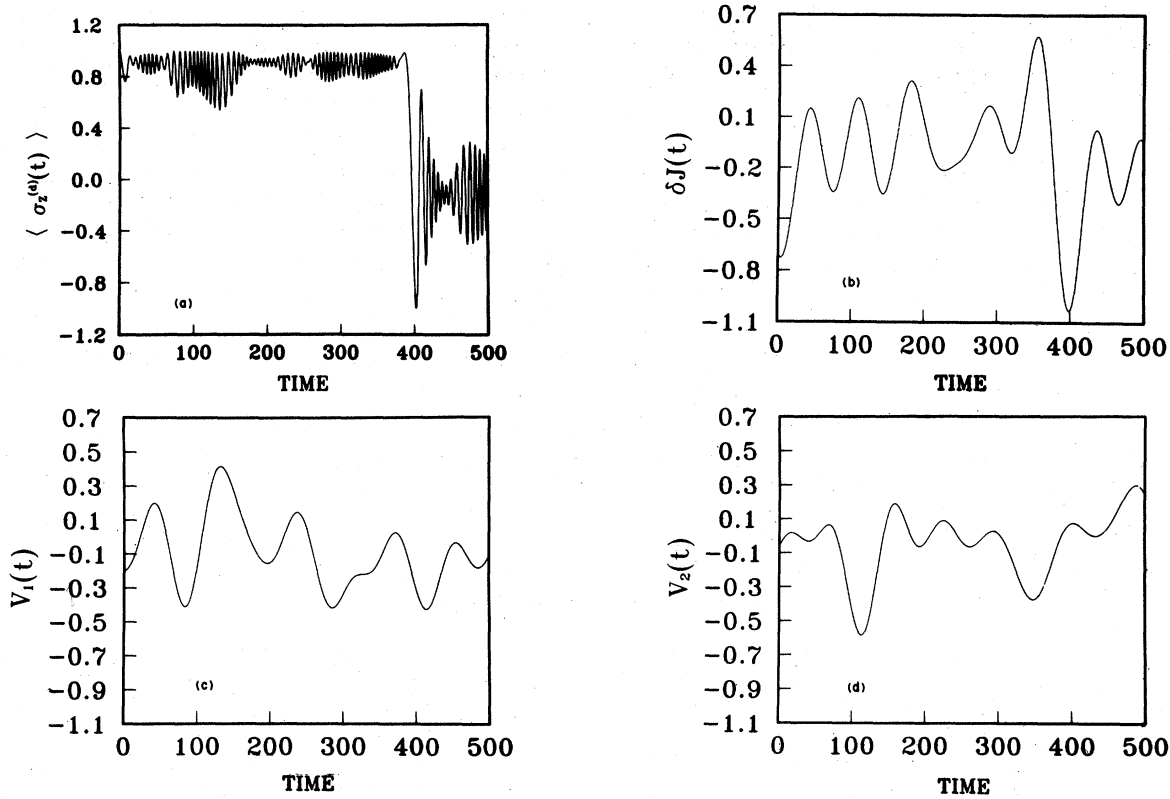


FIG. 3. Numerical solution of Eq. (3.4) with  $\omega_0=1.0$ ,  $\omega=0.1$ ,  $\langle \delta J_S^2 \rangle^{1/2}=1.5$ , and  $\langle V_{1,2}^2 \rangle_s^{1/2}=1.0$ . (a) Population difference  $\langle \vec{\sigma}_z^{(d)}(t) \rangle$ , (b)  $\delta J(t)$ , (c)  $V_1(t)$ , (d)  $V_2(t)$ .

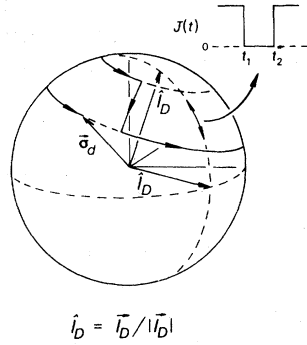


FIG. 4. Elementary picture of dynamics on the Bloch sphere for the crossing event illustrated by Fig. 3. Unit vector  $\hat{I}_D$  changes direction instantaneously at  $t_1$  and  $t_2$ .

virtual transitions and therefore have no direct bearing on the nonadiabatic capture rate. However, their dynamical significance has already been recognized; the ratio between the period of these nutations— $\sim 2\pi/\bar{\lambda}$ —and the typical period of lattice vibrations— $\sim 2\pi/\omega_M$ —determines the nonadiabatic coupling strength [Eq. (3.17)]. Also, computationally their importance is paramount, since this shortest timescale decides the time step for the integration routine. A great saving in computation time would be made if the need to follow these oscillations could be avoided. This is particularly important as we contemplate stochastic averaging, where many separate solutions must be generated.

A second time scale evidenced in Fig. 3(a) correlates with the fluctuations in  $\delta J(t)$  and  $V(t)$ . Here, as  $\vec{I}_D$  wanders the Bloch sphere its projection on the  $z$  axis contributes a low-frequency component to  $\langle \vec{\sigma}_z^{(d)}(t) \rangle$ . Modulations in the period and amplitude of the precessional oscillations accompany the motion of  $\vec{I}_D$ . For the most part the behavior is near-adiabatic. However, at  $t \approx 400$ , a manifestly

nonadiabatic event arises in conjunction with a crossing in  $J(t)$ . This transition represents neither the near-adiabatic nor the near-sudden limit, both of which bring only small changes to the population difference. We may offer a qualitative understanding through the simplified dynamics illustrated in Fig. 4. Let us simulate  $J(t)$  by sudden approximations at  $t_1$  and  $t_2$  as shown. In the interval  $t_1 < t_2$ ,  $J(t) = 0$ , and  $\vec{I}_D$  lies in the  $(x_d, y_d)$  plane [Eq. (3.6)]. If  $\bar{\lambda}_c$  is the precession frequency averaged throughout the crossing, we require

$$\Delta t = t_2 - t_1 \sim \frac{2\pi}{\omega_M} < \frac{2\pi}{\bar{\lambda}_c}.$$

Generally,  $\bar{\lambda} \gg \omega_M$  ( $\omega_0 = 10\omega_M$ ) and here  $\bar{\lambda}_c < \omega_M$  reflects the slowed precessional response with  $J = 0$ . Then the Bloch trajectory in Fig. 4 corresponds to adiabatic solution for three intervals— $t < t_1$ ,  $t_1 < t < t_2$ , and  $t_2 < t$ —where, in each,  $J$  and  $V$  are taken constant. Note that the phase with which  $\vec{\sigma}_d$  enters a crossing is important for its outcome. Depending on this phase,  $\langle \vec{\sigma}_z^{(d)}(t) \rangle$  may either decrease, as in Fig. 3(a), or increase. A thorough discussion, devoted solely to these crossing events, is planned for separate publication.

We have already mentioned the numerical difficulties which arise with the oscillatory adiabatic response. This problem has motivated our consideration of Eqs. (3.15) and (4.12) for integrating through the regions of near-adiabatic dynamics between crossing events. In Fig. 5 we have plotted zeroth-order solutions following from these equations for comparison with the solution in Fig. 3. We would not expect to replicate this result beyond the crossing, and here the departure of both approximations from the exact solution is obvious.<sup>36</sup> However, agreement before this event is generally good.

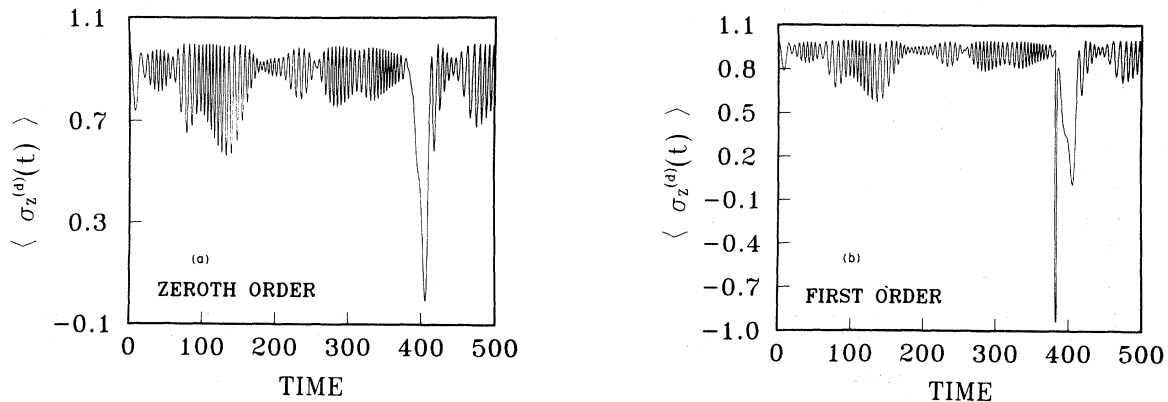


FIG. 5. Solution of Eq. (3.4) for the stochastic realization plotted in Fig. 3 using (a) the zeroth-order (adiabatic) approximation of Eq. (3.15), and (b) the first-order approximation of Eq. (4.14).

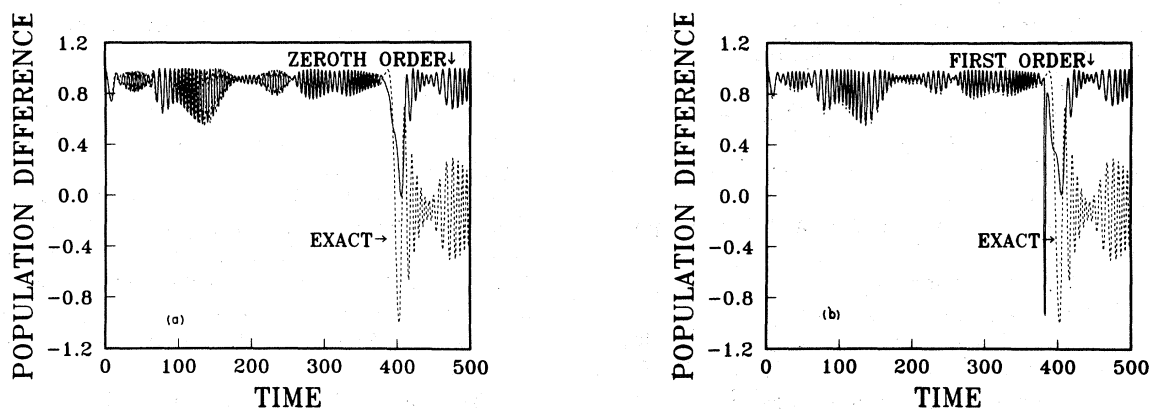


FIG. 6. (a) and (b): Approximate solutions of Eq. (3.4) from Figs. 5(a) and 5(b) superposed with the exact result from Fig. 3(a).

To aid in this comparison the approximate and exact results are superposed in Fig. 6. Errors of up to  $\sim 65\%$  can be found in the adiabatic solution, which is at times a full half-cycle out of phase with the correct result. Equation (4.12) brings significant improvement, with the errors typically reduced by an order of magnitude.

Efrima and Bixon<sup>37</sup> have considered the problem of electron exchange reactions in a stochastic solvent. Since they treat their problem in a two-level approximation, with the interaction represented as a random  $2 \times 2$  matrix, their problem is formally identical to ours. They treat the problem only in what they call a nonadiabatic approximation. Their treatment, however, treats the off-diagonal interaction as weak. The weak-coupling procedure can be carried out explicitly, and was one of the analytic procedures reported in our earlier work.<sup>31</sup> Indeed their procedure can be shown to lead to identical results as those previously obtained.<sup>31</sup>

## VI. SUMMARY

We have formulated a two-level semiclassical model for studying the nonadiabatic character of radiationless transitions in solids and give numerical results illustrating the dynamical content of this model. An effort has been made to give an intuitive view of nonadiabatic dynamics and to this end we have proposed the magnetic analogy discussed in Sec. III. Here lattice dynamics are identified with a

fluctuating magnetic field and the electronic state is represented by a precessing magnetic moment. A nonadiabatic response to changes in the direction of the magnetic field now provides the mechanism for transitions. Energy-level crossings slow precessional oscillations and limit the capacity for adiabatic following.

For near-adiabatic behavior we have obtained an analytic solution including nonadiabatic effects to first order. Our design is to use this solution to speed up the numerical procedures involved in a Monte Carlo calculation of capture rates. A comparison with exact numerical results has therefore been made, and this typically shows improvement by an order of magnitude over the adiabatic approximation.

An understanding of radiationless transition in experimental systems can come only with the accurate determination of the variables which characterize crossing events. The nonadiabatic mechanism may potentially be employed over a range from near-adiabatic limit to the near-sudden limit. In our further study of the model described here we hope to characterize capture processes throughout this range.

## ACKNOWLEDGMENT

The work at City College was supported in part by a Grant from the Department of Energy and the Army Research Office.

<sup>1</sup>M. Lax, *J. Phys. Chem. Solids* **8**, 66 (1959); *Phys. Rev.* **119**, 1502 (1960).

<sup>2</sup>E. F. Smith and P. T. Landsberg, *J. Phys. Chem. Solids* **27**, 1727 (1966).

<sup>3</sup>H. I. Ralph and F. D. Hughes, *Solid State Commun.* **2**, 1477 (1971).

<sup>4</sup>S. Koenig, *Phys. Rev.* **110**, 986 (1958).

<sup>5</sup>P. T. Landsberg, *Phys. Status Solidi* **41**, 457 (1970).

- <sup>6</sup>For a general review and references, see R. Englman, *Non-Radiative Decay of Ions and Molecules in Solids* (North-Holland, Amsterdam, 1979).
- <sup>7</sup>D. F. Nelson, J. D. Cuthbert, P. J. Dean, and G. D. Thomas, *Phys. Rev. Lett.* **17**, 1262 (1966).
- <sup>8</sup>P. J. Dean, R. A. Faulkner, S. Kimura, and M. Ilegems, *Phys. Rev. B* **4**, 1926 (1971).
- <sup>9</sup>J. S. Jayson, R. N. Bhargava, and R. W. Dixon, *J. Appl. Phys.* **41**, 4972 (1970).
- <sup>10</sup>M. Jaros, *Solid State Commun.* **25**, 1071 (1978).
- <sup>11</sup>R. Williams, *J. Appl. Phys.* **37**, 3411 (1966).
- <sup>12</sup>C. T. Sah, L. Forbes, L. L. Rosier, and A. F. Tasch, Jr., *Solid-State Electron.* **13**, 759 (1970); C. T. Sah, W. W. Chan, H. S. Fu, and J. W. Walker, *Appl. Phys. Lett.* **20**, 193 (1972).
- <sup>13</sup>H. Kukimoto, C. H. Henry, and F. R. Merritt, *Phys. Rev. B* **7**, 2486 (1973); C. H. Henry, H. Kukimoto, G. L. Miller, and F. R. Merritt, *ibid.* **7**, 2499 (1973).
- <sup>14</sup>D. V. Lang, *J. Appl. Phys.* **45**, 3014 (1974); **45**, 3023 (1974).
- <sup>15</sup>D. L. Losee, *Appl. Phys. Lett.* **21**, 54 (1972).
- <sup>16</sup>M. Schulz, *Appl. Phys.* **4**, 91 (1974).
- <sup>17</sup>D. V. Lang and C. H. Henry, *Phys. Rev. Lett.* **35**, 1525 (1975).
- <sup>18</sup>C. H. Henry and D. V. Lang, *Phys. Rev. B* **15**, 989 (1977).
- <sup>19</sup>V. Narayanamurti, R. A. Logan, and M. A. Chin, *Phys. Rev. Lett.* **40**, 63 (1978).
- <sup>20</sup>R. Englman and J. Jortner, *Mol. Phys.* **18**, 145 (1969).
- <sup>21</sup>R. Kubo and Y. Toyozawa, *Prog. Theor. Phys.* **13**, 160 (1955).
- <sup>22</sup>G. Rickayzen, *Proc. R. Soc. London Ser. A* **241**, 480 (1957).
- <sup>23</sup>K. Huang and A. Rhys, *Proc. R. Soc. London Ser. A* **204**, 406 (1950).
- <sup>24</sup>M. Lax, *J. Chem. Phys.* **20**, 1752 (1952).
- <sup>25</sup>M. Lax and E. Burstein, *Phys. Rev.* **100**, 592 (1955).
- <sup>26</sup>H. Gummel and M. Lax, *Phys. Rev.* **97**, 1469 (1955); *Ann. Phys. (N.Y.)* **2**, 28 (1957).
- <sup>27</sup>V. A. Kovarskii, *Fiz. Tverd. Tela (Leningrad)* **4**, 1636 (1962) [*Sov. Phys.—Solid State* **4**, 1200 (1962)]; V. A. Kovarskii and E. P. Sinyavskii, *ibid.* **4**, 3202 (1962) [*ibid.* **4**, 2345 (1963)]; **6**, 636 (1964) [**6**, 498 (1964)].
- <sup>28</sup>E. P. Sinyavskii and V. A. Kovarskii, *Fiz. Tverd. Tela (Leningrad)* **9**, 1464 (1967) [*Sov. Phys.—Solid State* **9**, 1142 (1967)].
- <sup>29</sup>B. Sharf and R. Silbey, *Chem. Phys. Lett.* **4**, 423 (1969); **4**, 561 (1970); **9**, 125 (1971).
- <sup>30</sup>A. Nitzan and J. Jortner, *J. Chem. Phys.* **56**, 3360 (1972).
- <sup>31</sup>M. Lax and W. J. Shugard, in *Statistical Mechanics and Statistical Methods in Theory and Application*, edited by U. Landman (Plenum, New York, 1977), pp. 429–439.
- <sup>32</sup>L. D. Landau and E. M. Lifshitz, *Quantum Mechanics* (Pergamon, Elmsford, N. Y., 1958), p. 305.
- <sup>33</sup>C. Zener, *Proc. R. Soc. London Ser. A* **137**, 696 (1932).
- <sup>34</sup>L. Allen and J. H. Eberly, *Optical Resonance and Two-Level Atoms* (Wiley, New York, 1975).
- <sup>35</sup>H. Goldstein, *Classical Mechanics* (Addison-Wesley, Reading, Mass., 1950), pp. 107–109.
- <sup>36</sup>If an exact integration procedure is employed at the crossing, an approximate scheme may again be taken up following its completion.
- <sup>37</sup>S. Efrima and M. Bixon, *J. Chem. Phys.* **70**, 3531 (1979).